

# DIGITAL MODELING OF STRING INSTRUMENT BRIDGE REFLECTANCE AND BODY RADIATIVITY FOR SOUND SYNTHESIS BY DIGITAL WAVEGUIDES

*Esteban Maestre*<sup>1,2,3\*</sup> *Gary P. Scavone*<sup>1</sup> *Julius O. Smith III*<sup>3</sup>

<sup>1</sup> Computational Acoustic Modeling Lab, McGill University, Canada

<sup>2</sup> Music Technology Group, Universitat Pompeu Fabra, Spain

<sup>3</sup> Center for Computer Research in Music and Acoustics, Stanford University, USA

## ABSTRACT

This paper proposes a method for modeling bridge reflectances and body radiativity profiles as digital filters in the context of sound synthesis by digital waveguides. The model is based on modal analysis of bridge driving-point admittance measurements obtained experimentally. Digital filter coefficients are estimated from modal analysis parameters, which are obtained by an optimization process that minimizes the error between measured and synthesized admittances, and between measured and synthesized radiativity profiles. Filter coefficients are then used in a digital waveguide synthesis model to render plucked string sounds.

**Index Terms**— String instrument, bridge, admittance, radiativity, digital filter, modal synthesis, digital waveguides

## 1. INTRODUCTION

String instruments radiate sound indirectly: energy from a narrow vibrating string is transferred to a radiation-efficient body of larger surface area. To a large extent, sound radiation is produced due to the transverse velocity of the instrument body surfaces (e.g., the front or back plates), and such surface motion is transferred to the body through the force that the string exerts on the instrument's bridge. Because of the importance of the bridge in mechanically coupling the strings and the body, the relation between applied force and both the induced velocity at the bridge and the radiated sound has been an object of study for over forty years [1].

Focusing on sound synthesis methods that do not rely on expensive convolutions with measured impulse responses, an early work on efficient digital modeling of bridge admittances for sound synthesis [2] proposed and evaluated several techniques for automatic design of common-denominator IIR filter parameters from violin bridge admittance measurements, making real-time violin synthesis an affordable task by combining digital filters with digital waveguides. However, while efficiency and accuracy can be well accomplished (also when applied to other string instruments [3]), positive-realness (passivity) [4] cannot be easily guaranteed with common-denominator IIR schemes, leading to instability problems when used to build string terminations. In that regard, using the modal framework [5] as a strategy for designing IIR filters offers two advantages: (i) admittance can be represented through a physically meaningful formulation, and (ii) positive-realness can be enforced. Less efficient approaches for admittance modeling are based on classical modal synthesis or frequency-domain methods [6]. Radiativity profiles are easier to measure because they can be acquired with sound pressure transducers, as opposed to mechanical vibration

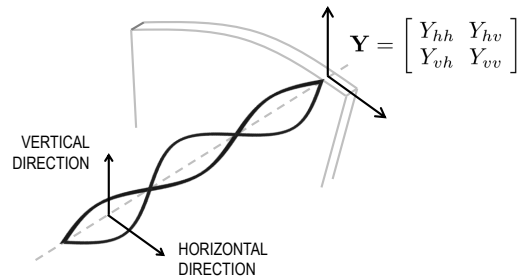


Figure 1: Two-dimensional bridge driving-point admittance.

transducers. Measured radiativity profiles have traditionally served [7, 8] as a musical instrument analysis technique.

Our work is focused on efficient sound synthesis by using the digital waveguide<sup>1</sup> framework [9]. The traveling wave solution of the homogeneous wave equation is used to model each transversal direction of motion of an ideal string. This is efficiently implemented by bi-directional digital delay lines holding velocity traveling waves, one per string and transversal direction. We ignore wave dispersion due to bending stiffness. Propagation losses are consolidated at the end of each delay line and implemented with a first-order recursive digital filter. Starting from experimental measurements of bridge admittance and body radiativity, this paper is concerned with the design of lumped string terminations that efficiently model wave reflectance at the bridge, string-string coupling at the bridge, and sound radiativity. Our models are based on a modal decomposition of the bridge input admittance, which is then used as a basis to design said terminations as digital filters in parallel form.

The paper is organized as follows. Section 2 reviews the technique used to obtain a modal decomposition of the bridge input admittance from vibration measurements. Following the digital waveguide theory for lumped junctions, Section 3 introduces a bridge reflectance formulation that allows the direct interconnection of any number of waveguides and also obtaining the bridge force. In Section 4, we propose a model for radiativity that is constructed by fitting radiativity measurements to a projection of the modal decomposition of the bridge input admittance. Two models are proposed for radiativity: a first, simpler model is based on a real-valued projection over the admittance modal basis; a second, more elaborated model is based on a complex-valued projection over the admittance modal basis, requiring a reformulation of the reflectance model. Section 5 concludes the paper by presenting some results and showing directions for future work.

\*Thanks to the European Research Council for funding.

<sup>1</sup><http://ccrma.stanford.edu/~jos/wg.html>

## 2. MODAL ANALYSIS OF THE BRIDGE ADMITTANCE

We model the two-dimensional driving-point bridge admittance matrix  $\mathbf{Y}$  of Figure 1 via the modal framework, by means of an IIR digital filter in parallel form. Starting from the passive admittance matrix formulation introduced in [10] (see equation (1)), we developed an optimization technique for fitting the parameters of a passive IIR digital filter to vibration measurements obtained experimentally.

A useful set of structurally passive two-dimensional driving-point admittance matrices are expressed in the  $z$ -domain [10] as

$$\hat{\mathbf{Y}}(z) = \begin{bmatrix} \hat{Y}_{hh}(z) & \hat{Y}_{hv}(z) \\ \hat{Y}_{hv}(z) & \hat{Y}_{vv}(z) \end{bmatrix} = \sum_{m=1}^M H_m(z) \mathbf{R}_m, \quad (1)$$

where each  $\mathbf{R}_m$  is a  $2 \times 2$  positive semidefinite matrix, and each  $m$ -th scalar modal response

$$H_m(z) = \frac{1 - z^{-2}}{(1 - p_m z^{-1})(1 - p_m^* z^{-1})}$$

is a second-order resonator determined by a pair of complex conjugate poles  $p_m$  and  $p_m^*$ . The numerator  $1 - z^{-2}$  is the bilinear-transform image of  $s$ -plane zeros at DC and infinity, respectively, arising under the ‘‘proportional damping’’ assumption [11]. It can be checked that  $H_m(z)$  is positive real for all  $|p_m| < 1$  (stable poles). We estimate  $p_m$  in terms of the natural frequency and the *half-power* bandwidth of the  $m$ -th resonator [4].

Departing from admittance measurements in digital form and the  $M$ -th order modal decomposition described in equation (1), the modal estimation problem is posed as the constrained minimization

$$\begin{aligned} & \underset{\omega, \mathbf{B}, \mathbf{R}}{\text{minimize}} && \mathcal{E}(\mathbf{Y}, \hat{\mathbf{Y}}) \\ & \text{subject to} && \mathbf{C}, \end{aligned} \quad (2)$$

where  $\omega = \{\omega_1, \dots, \omega_M\}$  are the modal natural frequencies,  $\mathbf{B} = \{B_1, \dots, B_M\}$  are the modal bandwidths,  $\mathbf{R} = \{\mathbf{R}_1, \dots, \mathbf{R}_M\}$  are the gain matrices,  $\mathcal{E}(\mathbf{Y}, \hat{\mathbf{Y}})$  is the error between the measurement matrix  $\mathbf{Y}$  and the model matrix  $\hat{\mathbf{Y}}$ , and  $\mathbf{C}$  is a set of constraints.

In a first stage, mode frequencies and bandwidths are estimated in the frequency domain via sequential quadratic programming [12]. Then, mode amplitudes are estimated via semidefinite programming [12] while enforcing passivity. We obtain accurate, low-order digital admittance matrix models relying on the modal framework. The frequency response of the horizontal entry  $\hat{Y}_{hh}$  of a cello bridge admittance matrix model ( $M = 15$ ) is displayed in Figure 2. Details about this modeling procedure, including both the measurement and the fitting, can be found in [13].

## 3. REFLECTANCE MODEL

Following the digital waveguide formulation for loaded junctions [4], let  $\mathbf{v}_n^+(n)$  and  $\mathbf{v}_n^-(n)$  respectively be the vectors of incoming and outgoing transversal velocity waves (in our case, each vector is two-dimensional) from the  $n$ -th string connected to the bridge. Analogously, let  $\mathbf{f}_n^+(n)$  and  $\mathbf{f}_n^-(n)$  be the vectors of incoming and outgoing transversal force waves of the  $n$ -th string acting on the bridge. The transversal velocity  $\mathbf{v}_n(n)$  and force  $\mathbf{f}_n(n)$  of the  $n$ -th string at the bridge are  $\mathbf{v}_n(n) = \mathbf{v}_n^+(n) + \mathbf{v}_n^-(n)$  and  $\mathbf{f}_n(n) = \mathbf{f}_n^+(n) + \mathbf{f}_n^-(n)$ .

Being a series connection for transverse waves, the bridge and the endpoints of the  $N$  strings present the same velocity at all times,

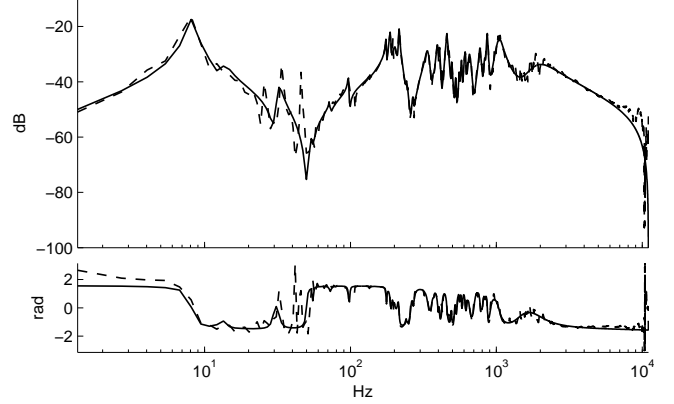


Figure 2: Example fitting results of cello bridge horizontal admittance entry  $\hat{Y}_{hh}$ . Magnitude (top) and phase (bottom). Sampling frequency of 22050 Hz. Dashed curves: admittance measurement; solid curves: model synthesized with  $M = 27$ .

while the total sum of string forces must equal that of the bridge. This yields

$$\mathbf{v}_B(n) = \mathbf{v}_1(n) = \dots = \mathbf{v}_N(n)$$

and

$$\mathbf{f}_B(n) = \sum_{n=1}^N \mathbf{f}_n(n),$$

with  $\mathbf{v}_B(n)$  and  $\mathbf{f}_B(n)$  being the bridge velocity and force vectors respectively. In the  $z$ -domain, it can be proved that

$$\mathbf{F}_B(z) = \frac{2 \sum_{n=1}^N \mathbf{Z}_n \mathbf{V}_n^+(z)}{1 + \mathbf{Z}_T^T \mathbf{Y}_B(z)}, \quad (3)$$

where  $\mathbf{Z}_n$  is a diagonal matrix representing the wave impedance of the  $n$ -th string,

$$\mathbf{Z}_T = \sum_{n=1}^N \mathbf{Z}_n,$$

and  $\mathbf{Y}_B(z)$  is the  $z$ -domain expression for the model of the driving-point admittance (see  $\hat{\mathbf{Y}}(z)$  in equation (1)). From the bridge force vector  $\mathbf{F}_B(z)$ , it should be straightforward to compute the bridge velocity vector  $\mathbf{V}_B(z)$  via

$$\mathbf{V}_B(z) = \mathbf{Y}_B(z) \mathbf{F}_B(z). \quad (4)$$

Back in the time domain, from the bridge velocity vector  $\mathbf{v}_B(n)$  it is possible to obtain the outgoing velocity wave vectors by means of

$$\mathbf{v}_n^-(n) = \mathbf{v}_B(n) - \mathbf{v}_n^+(n). \quad (5)$$

### 3.1. Parallel reflectance model

Because the formulation of the bridge driving-point admittance  $\mathbf{Y}_B(z)$  presents a parallel structure (see equation (1)) that we want to maintain in our implementation, inverting  $\mathbf{Y}_B(z)$  as it appears in equation (3) is impractical (the parallel structure would be lost). This problem can be overcome by reformulating each scalar modal response  $H_m(z)$  in equation (1) as proposed in [14], and later applied in [10], using wave-digital parallel adaptors to interconnect

multiple string (waveguide) terminations. Here we follow a similar procedure (via applying the reformulation of second-order sections as introduced in [14]) though instead of using wave-digital parallel adaptors to interconnect multiple waveguides at the bridge, we propose a new reflectance formulation that enables direct attachment of any number of waveguide terminations and, most importantly, obtaining the bridge force  $\mathbf{F}_B(z)$ .

First, let's revisit the reformulation of second-order sections as introduced in [14] and applied in [10]. Let each scalar modal response  $H_m(z)$  in  $\mathbf{Y}_B(z)$  be expressed as

$$H_m(z) = \frac{1 - z^{-2}}{1 + a_{m,1}z^{-1} + a_{m,2}z^{-2}}, \quad (6)$$

where  $a_{1,m} = -2|p_m| \cos(\angle p_m)$  and  $a_{2,m} = |p_m|^2$ . It is possible to re-write  $H_m(z)$  as

$$H_m(z) = 1 + z^{-1}H_m^p(z) = 1 + z^{-1} \frac{b_{m,0} + b_{m,1}z^{-1}}{1 + a_{m,1}z^{-1} + a_{m,2}z^{-2}}, \quad (7)$$

where  $b_{m,0} = -a_{m,1}$  and  $b_{m,1} = -1 - a_{m,2}$ . The expression for  $\mathbf{Y}_B(z)$  becomes

$$\mathbf{Y}_B(z) = \mathbf{Y}_B^i + z^{-1}\mathbf{Y}_B^p(z), \quad (8)$$

with

$$\mathbf{Y}_B^i = \sum_{m=1}^M \mathbf{R}_m \quad (9)$$

$$\mathbf{Y}_B^p(z) = \sum_{m=1}^M H_m^p(z) \mathbf{R}_m.$$

Our proposed solution to the problem of formulating a reflectance is to plug the reformulated admittance model of equation (8) into equations (3) and (4) as follows. We first re-write equation (3) as

$$\mathbf{F}_B(z) + \mathbf{Z}_T \mathbf{Y}_B(z) \mathbf{F}_B(z) = 2 \sum_{n=1}^N \mathbf{Z}_n \mathbf{V}_n^+(z) \quad (10)$$

and, by using equation (8) and solving for the bridge force vector  $\mathbf{F}_B(z)$ , we obtain

$$\mathbf{F}_B(z) = \frac{2 \sum_{n=1}^N \mathbf{Z}_n \mathbf{V}_n^+(z) - z^{-1} \mathbf{Z}_T \mathbf{Y}_B^p(z) \mathbf{F}_B(z)}{1 + \mathbf{Z}_T \mathbf{Y}_B^i}. \quad (11)$$

Then, introducing equation (8) into equation (4), the expression for the bridge velocity vector  $\mathbf{V}_B(z)$  becomes

$$\mathbf{V}_B(z) = \mathbf{Y}_B^i \mathbf{F}_B(z) + z^{-1} \mathbf{Y}_B^p(z) \mathbf{F}_B(z). \quad (12)$$

#### 4. RADIATIVITY MODEL

By using a calibrated force hammer (impact at the bridge, in the vertical and horizontal directions) and a sound pressure transducer (microphone at 1.5m distance facing the top plate), we measured radiativity frequency responses by deconvolving the measured sound pressure signal by the input excitation force signal. Measured frequency responses are  $D_h(\omega)$  and  $D_v(\omega)$ , for horizontal and vertical bridge excitation respectively. Our assumption is that, considering a two-dimensional model for the bridge admittance, the total sound pressure  $P$  at the microphone will be the sum of the contributions from the two directions (horizontal and vertical) of the bridge force.

#### 4.1. Model with real gains

Our aim is to construct a digital filter  $\mathbf{E}(z)$  such that the modeled sound pressure signal  $\hat{P}(z)$  can be obtained during synthesis as

$$\hat{P}(z) = \mathbf{E}(z) \mathbf{F}_B(z), \quad (13)$$

where  $\mathbf{F}_B(z) = [F_{B,h}(z) F_{B,v}(z)]^T$  is the bridge force vector and  $\mathbf{E}(z) = [E_h(z) E_v(z)]$  is constructed from two transfer functions, each dedicated to one direction of force at the bridge. By taking advantage of the modal estimation that was carried out when modeling the admittance [13] we propose first a model for each transfer function  $E(z)$  in  $\mathbf{E}(z)$  as

$$E(z) = \sum_{m=1}^M H_m(z) \gamma_m, \quad (14)$$

where  $\gamma_m$  is a real-valued scalar used to weight the  $m$ -th mode. In order to estimate the gains  $\gamma_m$ , we solve the linear problem

$$\underset{\boldsymbol{\gamma}}{\text{minimize}} \|\mathbf{B}\boldsymbol{\gamma} - \mathbf{d}\|, \quad (15)$$

where  $\boldsymbol{\gamma} = [\gamma_1 \cdots \gamma_m \cdots \gamma_M]^T$  is a real-valued gain vector,  $\mathbf{B}$  is a matrix (basis) with each  $m$ -th column containing samples of the impulse response of  $H_m(z)$ , and  $\mathbf{d}$  is a vector containing samples of the impulse response of measurement  $D$ . In other words, we project the measured microphone onto the mode responses.

#### 4.2. Model with complex gains

To allow for complex gains and therefore any relative phase between modes, we model each of the scalar modal components of the radiation as the real damped oscillation that results from summing two complex resonators whose poles and residues respectively form complex-conjugate pairs [4]. It is possible to reformulate the reflectance model so that resulting second-order sections can be reused in the radiativity model, therefore minimizing the computational cost required by using complex gains in our radiativity model.

##### 4.2.1. Parallel reflectance model

Here we present an alternate method for formulating the parallel admittance model so that it is possible to use a single set of second order sections in both the reflectance and radiativity models. First, we proceed to express the admittance expression in equation (1) as

$$\mathbf{Y}(z) = (1 - z^{-2}) \sum_{m=1}^M U_m(z) \mathbf{R}_m, \quad (16)$$

where  $\mathbf{R}_m$  is a positive semidefinite matrix, and each scalar

$$U_m(z) = \frac{1}{1 + a_{m,1}z^{-1} + a_{m,2}z^{-2}}, \quad (17)$$

has real coefficients, with  $a_{1,m} = -2|p_m| \cos(\angle p_m)$  and  $a_{2,m} = |p_m|^2$ . We reformulate each scalar  $U_m(z)$  as

$$U_m(z) = 1 + z^{-1}U_m^p(z) = 1 + z^{-1} \frac{c_{m,0} + c_{m,1}z^{-1}}{1 + a_{m,1}z^{-1} + a_{m,2}z^{-2}}, \quad (18)$$

where  $c_{m,0} = -a_{m,1}$  and  $c_{m,1} = -a_{m,2}$ . Now the expression for the bridge driving-point admittance matrix  $\mathbf{Y}_B(z)$  can be written as

$$\mathbf{Y}_B(z) = (1 - z^{-2})(\mathbf{Y}_B^i + z^{-1}\mathbf{Y}_B^p(z)), \quad (19)$$

where

$$\begin{aligned} \mathbf{Y}_B^i &= \sum_{m=1}^M \mathbf{R}_m \\ \mathbf{Y}_B^q(z) &= \sum_{m=1}^M U_m^p(z) \mathbf{R}_m. \end{aligned} \quad (20)$$

In an analogous manner as introduced in Section 3, we use equations (10), (12), and (19) to derive the  $z$ -domain expressions needed for our reflectance model (the  $z$  arguments have been dropped for notational simplicity):

$$\mathbf{F}_B = \frac{2 \sum_{n=1}^N \mathbf{Z}_n \mathbf{V}_n^+ + z^{-2} \mathbf{Z}_T \mathbf{Y}_B^i \mathbf{F}_B - z^{-1} (1 - z^{-2}) \mathbf{Z}_T \mathbf{Y}_B^q \mathbf{F}_B}{1 + \mathbf{Z}_T \mathbf{Y}_B^i} \quad (21)$$

$$\mathbf{V}_B = (1 - z^{-2}) (\mathbf{Y}_B^i \mathbf{F}_B + z^{-1} \mathbf{Y}_B^q \mathbf{F}_B) \quad (22)$$

#### 4.2.2. Radiativity model

With our new formulation for the second order sections in the reflectance model, we can model each transfer function  $E(z)$  from  $\mathbf{E}(z)$  in equation (13) as

$$E(z) = \sum_{m=1}^M \frac{\eta_{0,m} + \eta_{1,m} z^{-1}}{1 + a_{1,m} z^{-1} + a_{2,m} z^{-2}}, \quad (23)$$

where  $\eta_{0,m}$  and  $\eta_{1,m}$  are real. Each  $m$ -th term in the sum has real coefficients and corresponds to the result of adding two complex resonators with respective poles and residues being complex-conjugate. Each  $m$ -th pair of complex poles  $p_m$  and  $p_m^*$  leads to denominator terms  $a_{1,m} = -2|p_m| \cos(\angle p_m)$  and  $a_{2,m} = |p_m|^2$ . Using equation (17), we can write

$$E(z) = \sum_{m=1}^M (\eta_{0,m} + \eta_{1,m} z^{-1}) U_m(z). \quad (24)$$

Vectors  $\boldsymbol{\eta}_0 = [\eta_{0,1} \cdots \eta_{0,m} \cdots \eta_{0,M}]^T$  and  $\boldsymbol{\eta}_1 = [\eta_{1,1} \cdots \eta_{1,m} \cdots \eta_{1,M}]^T$  can be obtained by solving the linear problem

$$\underset{\boldsymbol{\eta}}{\text{minimize}} \|\mathbf{B}\boldsymbol{\eta} - \mathbf{d}\|, \quad (25)$$

where  $\boldsymbol{\eta} = [\boldsymbol{\eta}_0^T \boldsymbol{\eta}_1^T]^T$  is a real-valued vector;  $\mathbf{d}$  is a vector containing samples of the impulse response of measurement  $D$ ; and  $\mathbf{B}$  is a matrix (basis) with each  $m$ -th of the first  $M$  columns containing samples of the impulse response of  $U_m(z)$ , and each  $m$ -th of the remaining  $M$  columns containing samples of the impulse response of  $z^{-1}U_m(z)$ .

## 5. CONCLUSION

This paper proposes a method for modeling bridge reflectances and body radiativity profiles as digital filters in the context of sound synthesis by digital waveguides. The technique, which is based on modal analysis of bridge driving-point admittance measurements, provides a basis for estimating digital filter coefficients by minimizing the error between measured and synthesized admittances, and between measured and synthesized radiativity profiles. Obtained

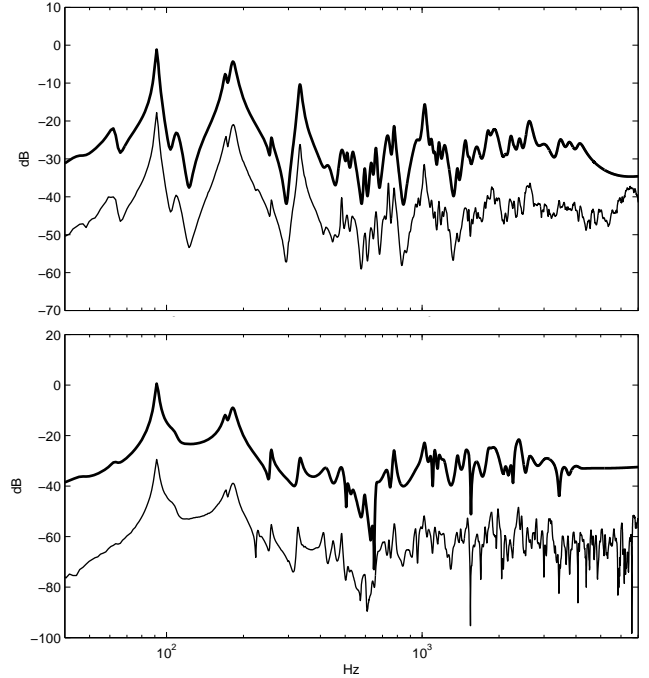


Figure 3: Guitar modeling example, with  $M = 36$  in the range  $40 < f < 5000$  Hz. Measured (thin line) versus synthesized (thick line) bridge horizontal admittance (top) and radiativity (bottom). Scaling was applied for clarity.

digital filter coefficients can be used to build an efficient sound synthesis model including bridge reflectance, measured radiativity, and (implicitly) lost vibrational energy from the bridge transmittance to non-radiating modes. In Figure 3, an example modeled one-dimensional guitar admittance and its radiativity profile are plotted along with experimental measurements. Both are rendered via the models in Section 4.2, i.e. via the formulation used to express the radiativity as a complex-valued projection over the admittance modal basis. Sound examples rendered using these models can be found online<sup>2</sup> for guitar, violin, viola, and cello. From a psychoacoustics perspective, listening tests could help exploring the trade-off between computational cost (order model) and perceived sound fidelity.

A problem of this modeling procedure arises from the fact that the modal parameters estimated from admittance measurements are used for modeling measured radiativity profiles. Low-energy modes present in the admittance measurement can be missed by the optimization method due to their small contribution to the error function, and it may be the case that some of these modes turn out to be radiation-efficient. For that reason, the radiativity model may lack some prominent resonances in some cases. In the near future, we hope to improve on this aspect and also to explore the possibilities of using a spherical modal basis in our radiativity model.

## 6. ACKNOWLEDGMENT

Authors thank Charalampos Saitis for interesting discussions, and Hossein Mansour for providing additional guitar measurements.

<sup>2</sup><http://ccrma.stanford.edu/~esteban/reflrad/>

## 7. REFERENCES

- [1] T. Rossing, *The Science of String Instruments*. Springer New York, 2010.
- [2] J. O. Smith, “Techniques for digital filter design and system identification with application to the violin,” Ph.D. dissertation, Stanford University, 1983.
- [3] M. Karjalainen and J. O. Smith, “Body modeling techniques for string instrument synthesis,” in *Proc. of the International Computer Music Conference*, 1996.
- [4] J. O. Smith, *Physical Audio Signal Processing*. W3K Publishing, 2004. [Online]. Available: <http://cirma.stanford.edu/~jos/pasp/>
- [5] K. D. Marshall, “Modal analysis of a violin,” *Journal of the Acoustical Society of America*, vol. 77:2, pp. 695–709, 1985.
- [6] J. Woodhouse, “Plucked guitar transients: comparison of measurements and synthesis,” *Acta Acustica United with Acustica*, vol. 90:5, pp. 945–965, 2004.
- [7] N. H. Fletcher and T. D. Rossing, *The Physics of Musical Instruments, 2nd Edition*. New York: Springer Verlag, 1998.
- [8] G. Bissinger, “Structural acoustics model of the violin radiativity profile,” *J. Acoust. Soc. Am.*, vol. 124, pp. 4013–4023, 2008.
- [9] J. O. Smith, “Physical modeling using digital waveguides,” *Computer Music Journal*, vol. 16:4, pp. 74–91, 1992.
- [10] B. Bank and M. Karjalainen, “Passive admittance matrix modeling for guitar synthesis,” in *Proc. of the International Conference on Digital Audio Effects*, 2010.
- [11] J. Rayleigh, *The Theory of Sound vol. 1,2*. Macmillan, 1877-1878.
- [12] S. Boyd and L. Vandenberghe, *Convex Optimization*. Cambridge University Press, 2004. [Online]. Available: <http://www.stanford.edu/~boyd/cvxbook/>
- [13] E. Maestre, G. P. Scavone, and J. O. Smith, “Digital modeling of bridge driving-point admittances from measurements on violin family instruments,” in *Proc. of the Stockholm Music Acoustics Conference*, 2013.
- [14] M. Karjalainen, “Efficient realization of wave digital components for physical modeling and sound synthesis,” *IEEE Trans. Audio, Speech, and Lang. Process.*, vol. 16:5, pp. 947–956, 2008.